Anal. Chem. **2001,** *73,* 2078−2086

An Experimental Comparison of the Maximum Likelihood Estimation and Nonlinear Least-Squares Fluorescence Lifetime Analysis of Single Molecules

Michael Maus, Mircea Cotlet, Johan Hofkens,* Thomas Gensch, and Frans C. De Schryver

Division of Photochemistry and Spectroscopy, Department of Chemistry, Katholieke Universiteit Leuven, Celestijnenlaan 200F, 3001 Heverlee-Leuven, Belgium

J. Schaffer and C. A. M. Seidel*

Max-Planck-Institute for Biophysical Chemistry, Am Fassberg 11, D-37077 Göttingen, Germany

Two procedures based on the weighted least-squares (LS) and the maximum likelihood estimation (MLE) method to confidently analyze single-molecule (SM) fluorescence decays with a total number (*N*) of 2500−60 000 counts have been elucidated and experimentally compared by analyzing measured bulk and SM decays. The key observation of this comparison is that the LS systematically underestimates the fluorescence lifetimes by ∼5%, for the range of 1000−20 000 events, whereas the MLE method gives stable results over the whole intensity range, even at counts *N* less than 1000, where the LS analysis delivers unreasonable values. This difference can be attributed to the different statistics approaches and results from improper weighting of the LS method. As expected from theory, the results of both methods become equivalent above a certain threshold of *N* detected photons per decay, which is here experimentally determined to be ∼20 000. In contrast to the bulk lifetime distributions, the SM fluorescence lifetime distributions exhibit standard deviations that are sizably larger than the statistically expected values. This comparison proves the strong influence of the inhomogenuous microenvironment on the photophysical behavior of single molecules embedded in a 10−30-nm thin polymer layer.

Single-molecule (SM) detection using fluorescence microscopy has gained a rapidly increasing interest due to its inherent capabilities in analytical chemistry.[1−19] In particular, the analysis of SM decay times has been shown to be a very efficient way to distinguish between molecules of different chemical structures.[15−19] Since from single molecules only few fluorescence photons can be collected, the determination of the corresponding decay times requires precise and reproducible analysis procedures.

Some theoretical publications have pointed out that, for the fluorescence decay analysis, the most commonly used weighted least-squares (LS) method is insufficient to cope with the low number of counts in a decay histogram simply because the underlying assumption of a Gaussian instead of a Poissonian or multinominal distribution of errors is incorrect.[20−22] Nonetheless, the LS method is most widespread even for the analysis of SM fluorescence decays and thus renders the published values of SM

* Corresponding authors. J.H.: (fax) +32 16 327989; (e-mail) johan.hofkens@chem.kuleuven.ac.be. C.A.M.S.: (fax) +49 551 2011501; (e-mail) cseidel@gwdg.de.

(1) Meixner, A. Optical Single Molecule Detection at Room Temperature. In *Advances in Photochemistry*; Neckers, D. C., Volman, D. H., von Bünau, G., Eds.; John Wiley & Sons Inc.: New York, 1998; Vol 24.
(2) Nie, S.; Zare, R. N. *Annu. Rev. Biophys. Biomol. Struct.* **1997**, *26*, 567−596.
(3) Shera, E. B.; Seitzinger, N. K.; Davis, L. M.; Keller, R. A.; Soper, S. A. *Chem. Phys. Lett.* **1990**, *174*, 553−557.
(4) Barnes, M. D.; Whitten, W. B.; Ramsey, J. M. *Anal. Chem.* **1993**, *65*, 2360−2365.
(5) Rigler, R.; Mets, U.; Widengren, J.; Kask, P. *Eur. Biophys. J.* **1993**, *22*, 169−175.
(6) Nie, S.; Chiu, D. T.; Zare, R. N. *Science* **1994**, *266*, 1018−1021.
(7) Goodwin, P. M.; Ambrose, W. P.; Keller, R. A. *Acc. Chem. Res.* **1996**, *29*, 607−613.
(8) Zander, C.; Drexhage, K. H.; Han, K.-T.; Wolfrum, J.; Sauer, M. *Chem. Phys. Lett.* **1996**, *286*, 457−465.
(9) Chen, D.; Dovichi, N. J. *Anal. Chem.* **1996**, *68*, 690−696.
(10) Lyon, A.; Fang, M. M.; Haskins, W. E.; Nie, S. *Anal. Chem.* **1998**, *70*, 1743−1748.
(11) Simpson, P. C.; Roach, D.; Woolley, A. T.; Thorsen, T.; Johnston, R.; Sensabaugh, G. F.; Mathies, R. A. *Proc. Natl. Acad. Sci. U.S.A.* **1998**, *95*, 2256−2261.
(12) van Orden, A.; Machara, N. P.; Goodwin, P. M.; Keller, R. A. *Anal. Chem.* **1998**, *70*, 1444−1451.
(13) Schuetz, G. J.; Trabesinger, W.; Schmidt, T. *Biophys. J.* **1998**, *74*, 2223−2226.
(14) Kung, C.-Y.; Barnes, M. D.; Lermer, N.; Whitten, W. B.; Ramsey, J. M. *Anal. Chem.* **1998**, *70*, 658−661.
(15) Zander, C.; Sauer, M.; Drexhage, K. H.; Ko, D.-S.; Schulz, A.; Wolfrum, J.; Brand, L.; Eggeling, C.; Seidel, C. A. *Appl. Phys. B* **1996**, *63*, 517−523.
(16) Fries, J. R.; Brand, L.; Eggeling, C.; Köllner, M.; Seidel, C. A. M. *J. Phys. Chem. A* **1998**, *102*, 6601−6613.
(17) Müller, R.; Zander, C.; Sauer, M.; Deimel, M.; Ko, D.-S.; Siebert, S.; Arden-Jacob, J.; Deltau, G.; Marx, N. J.; Drexhage, K. H.; Wolfrum, J. *Chem. Phys. Lett.* **1996**, *262*, 716−722.
(18) Enderlein, J.; Goodwin, P. M.; Van Orden, A.; Ambrose, W. P.; Erdmann, R.; Keller, R. A. *J. Phys. Chem.* **1997**, *270*, 4464−470.
(19) Schaffer, J.; Volkmer, A.; Eggeling, C.; Subramaniam, V.; Striker, G.; Seidel, C. A. M. *J. Phys. Chem. A* **1999**, *103*, 331−336.
(20) Baker, S.; Cousins, R. D. *Nucl. Instrum. Methods* **1984**, *221*, 437−442.
(21) Hall, P.; Selinger, B. *J. Phys. Chem.* **1981**, *85*, 2941−2946.
(22) Bajzer, Z.; Therneau, J.; Sharp, C.; Prendergast, F. G. *Eur. Biophys. J.* **1991**, *20*, 247−262.

10.1021/ac000877g CCC: $20.00
Published on Web 04/04/2001

decay times questionable.[23−31] In case of bulk measurements, this problem does not appear, because at a high number of counts, the Poissonian and multinominal statistics converge to Gaussian statistics. A method that is purely based on the more appropriate multinominal statistics is the maximum likelihood estimation (MLE) method.[20−22] It was demonstrated that decays with a number of less than 10 counts in the maximum distributed over less than 200 channels, i.e., less than 200 total counts, can be analyzed by MLE, which is unambiguously impossible by a LS analysis.[15−19,32−35]

In several publications, the LS and MLE methods are theoretically compared[20−22] and the limits of the LS with the quality parameter reduced chi square, χ_r^2, and MLE with the quality parameter $2I_r$* have been investigated.[36−41] However, a literature research about SM fluorescence lifetime analysis revealed a lack of a LS−MLE comparison based on experimental SM data. Furthermore, many commercial software programs offer iterative χ_r^2 minimization routines for data analysis, which is not the case for routines based on $2I_r$*. Thus, it is our main aim to compare LS with MLE decay analysis of monoexponential SM fluorescence decays in order to point out that a quantitative systematic difference between the results of both methods exists. For these experiments, we upgraded our SM fluorescence spectroscopy setup with a time-resolved detection option and developed a MLE and LS decay analysis procedure. To ensure that unwanted experimental effects do not blur this comparison, attention has been given to the influence of channel number, background photons, number of photons collected per decay, and excitation polarization. As SM fluorophore, we used a highly fluorescent hexaphenylbenzene−perylenemonoimide dye that has been shown previously to obey a monoexponential fluorescence decay law.[42]Such a dye immobilized in a polymer film should exhibit decay times independent of the parameters mentioned above, particularly of the excitation polarization. The comparison of the mean lifetime obtained with linearly and circularly polarized excitation light has therefore been used to indicate the absence of experimental artifacts like photoselection and distortions due to anisotropy.

THEORY

The Fit Quality Parameters. The different statistical treatment of the LS compared with the MLE method can easily be revealed by a derivation of the likelihood function

$$L'(\boldsymbol{n},\boldsymbol{g}(\boldsymbol{x})) = \prod_{i=1}^{k} w\,(n_i,\boldsymbol{g}(\boldsymbol{x})) \tag{1}$$

where $w(n_i,\boldsymbol{g}(\boldsymbol{x}))$ represents the probability density that n_i counts in the ith channel of the experimental decay histogram $\boldsymbol{n} = (n_1,n_2,...,n_k)$ are detected. $\boldsymbol{n}$ is described by the proposed model expectation values $\boldsymbol{g} = (g_1(x),g_2(x),...,g_k(x))$ which itself result from the obtained fit parameter set $\boldsymbol{x}$, e.g., an amplitude α and a decay time τ of a monoexponential function. For the fitting procedure, it is convenient to apply the logarithm and to normalize the likelihood function $L'(\boldsymbol{n},\boldsymbol{g}(\boldsymbol{x}))$ with the likelihood of the absolutely exact "fit" $L'(\boldsymbol{n},\boldsymbol{n})$ such that the minimization of the negative logarithmic and normalized likelihood function which can be replaced by the MLE fit quality parameter $2I$*

$$-2lnL(\boldsymbol{n},\boldsymbol{g}) = -2\ln\prod_{i}^{k}\frac{w(n_i,\mathbf{g}(\mathbf{x}))}{w(n_i,n_i)} = -2\sum_{i}^{k}\ln\frac{w(n_i,\mathbf{g}(\mathbf{x}))}{w(n_i,n_i)} = 2I^* \tag{2}$$

leads to the most probable model parameter set $\mathbf{x}$ for the observed decay histogram $\boldsymbol{n}$.

If we assume now a superposition of a Gaussian noise to the signals n_i and introduce the standard deviation $\sigma_i = \sqrt{n_i}$, the probability density becomes

$$w(n_i,\boldsymbol{g}(\boldsymbol{x})) = \frac{1}{\sqrt{2\pi n_i}}e^{(n_i-g_i)^2/2n_i} \tag{3}$$

and by substitution of this eq 3 into eq 2 the relationship between the MLE fit quality parameter $2I$* in case of Gaussian distributed errors and the well-known chi square (χ^2) parameter becomes obvious:

$$2I^* = \sum_{i}^{k}\frac{(n_i - g_i)^2}{n_i} = \chi^2 \tag{4}$$

If the numbers of counts n_i in the k channels of the decay histogram are large, the Poissonian or multinominal is practically equal to the Gaussion distribution and hence the LS method based on fit minimizations with eq 4 is justified. However, for decays with a low number of counts as observed in some SM experiments, the more appropriate Poissonian or multinominal prob-

(23) Xie, X. S.; Dunn, R. C. *Science* **1994**, *265*, 361−364.
(24) Lu, H. P.; Xie, X. S. *J. Phys. Chem. B* **1997**, *101*, 2753−2757.
(25) Ying, L.; Xie, X. S. *J. Phys. Chem. B* **1998**, *102*, 10399−10409.
(26) Bopp, M. A.; Jia, Y.; Li, L.; Cogdell, R. J.; Hochstrasser, R. M. *Proc. Natl. Acad. Sci. U.S.A.* **1997**, *94*, 10630−10635.
(27) Jia, Y.; Sytnik, A.; Li, L.; Vladimirov, S.; Cooperman, B.; Hochstrasser, R. *Proc. Natl. Acad. Sci. U.S.A.* **1997**, *94*, 7932−7936.
(28) Macklin, J. J.; Trautmann, J. K.; Harris, T. D.; Brus, L. E. *Science* **1996**, *272*, 255−257.
(29) Ye, J. Y.; Ishikawa, M.; Yogi, O.; Okada, T.; Maruyama, Y. *Chem. Phys. Lett.* **1998**, *288*, 885−890.
(30) Ishikawa, M.; Yong Ye, J.; Maruyama, Y.; Nakatsuka, H. *J. Phys. Chem. A* **1999**, *103*, 4319−4331.
(31) An additional potential error source comes from the fact that some published SM decay times were analyzed without deconvolution of the instrument response function.
(32) Sauer, M.; Drexhage, K. H.; Lieberwirth, U.; Müller, R.; Nord, S.; Zander, C. *Chem. Phys. Lett.* **1998**, *284*, 153−163.
(33) Eggeling, C.; Fries, J. R.; Brand, L.; Günther, R.; Seidel, C. A. M. *Proc. Natl. Acad. Sci. U.S.A.* **1998**, *95*, 1556−1561.
(34) Soper, S. A.; Mattlingly, Q. L.; Vegunta, P. *Anal. Chem.* **1993**, *65*, 740−744.
(35) Brand, L.; Eggeling, C.; Zander, C.; Drexhage, K. H.; Seidel, C. A. M. *J. Phys. Chem. A* **1997**, *101*, 4313−4321.
(36) Grinvald, A.; Steinberg, I. *Anal. Biochem.* **1974**, *59*, 583−598.
(37) Tellinghuisen, J. *Anal. Chem.* **1993**, *65*, 1277−1280.
(38) Köllner, M.; Wolfrum, J. *Chem. Phys. Lett.* **1992**, *200*, 199−204.
(39) Köllner, M. *Appl. Opt.* **1993**, *32*, 806−820.
(40) Köllner, M.; Fischer, A.; Arden-Jacob, J.; Drexhage, K. H.; Müller, R.; Seeger, S.; Wolfrum, J. *Chem. Phys. Lett.* **1996**, *250*, 355−360.
(41) Tellinghuisen, J.; Wilkerson, C. W. *Anal. Chem.* **1993**, *65*, 1240−1246.
(42) Hofkens, J.; Latterini, L.; De Belder, G.; Gensch, T.; Maus, M.; Vosch, T.; Karni, Y.; Schweitzer, G.; De Schryver, F. C.; Herrmann, A.; Müllen, K. *Chem. Phys. Lett.* **1999**, *304*, 1−9.

ability distribution has to be considered for the true maximum likelihood estimation.[20−22] Moreover, the fact that the total number of counts $\sum n_i = N$ of a decay histogram is known from the measurement allows to apply directly the multinominal distribution. In this case, the probability density is given by

$$w(n_i,\boldsymbol{g}(\boldsymbol{x})) = (N!)^{1/k}\frac{{g_i}^{n_i}}{N^{n_i}n_i!} \tag{5}$$

which introduced to eq 2 yields the "true" likelihood relation

$$2I^* = 2\sum_i^k n_i \ln\frac{n_i}{g_i} \tag{6}$$

that is used as criterion for the minimization of the MLE fits. To get comparable fit quality parameters that are independent of the degrees of freedom determined by the number of analyzed channels k and by the number of fit parameters ν the reduced fit quality parameters

$${\chi_r}^2 = \sum_i^k \frac{(n_i - g_i)^2}{n_i(k-\nu)} \tag{7}$$

derived from eq 4 for the LS method and

$$2I_r^* = \frac{2}{k-\nu}\sum_i^k n_i \ln\frac{n_i}{g_i} \tag{8}$$

derived from eq 6 for the MLE method are introduced. Note that, for a simple monoexponential model function, the LS method uses $\nu = 2$ whereas the normalization of the decay histogram for the MLE method renders the estimation of the amplitude obsolete and reduces the degrees of freedom to $\nu = 1$.[43] The importance of the variance close to the calculated minimum (*Fisher information matrix*) and its bias has been stressed and derived in detail in several publications.[37−41,44] However, the bias is not crucial in the present work because the number of counts ($N > 3000$) in the analyzed decays is relatively large.

The Model Fit Function. The model fit function g_i for a single lifetime (τ) analysis in eq 9 is based on a monoexponential decay law which considers the convolution with an instrument response function (irf_i), the contribution of a known constant mean value (c) for the statistical noise of time-uncorrelated counts (dark noise of detector), and a possible contribution with a fraction γ of time-correlated background signal (bg_i) that can be induced by Rayleigh or Raman scatter or by fluorescence from the environment.

$$g_i = N_g\left[(1-\gamma)\frac{\mathrm{irf}_i \otimes \mathrm{e}^{iT/k\tau} + c}{\sum_{i=0}^{k}(\mathrm{irf}_i \otimes \mathrm{e}^{iT/k\tau} + c)} + \gamma\frac{\mathrm{bg}_i}{\sum_{i=0}^{k}\mathrm{bg}_i}\right] \tag{9}$$

For the fitting of the experimental decay histogram n_i to the model g_i in the time window T, the fluorescence lifetime τ, the background fraction γ, and the number of counts of the fit histogram N_g can be used as floating parameters. The basic difference between the MLE and LS method is that in case of LS analysis the amplitude N_g is variable, while for MLE N_g is not a fit parameter but is set equal to its actually measured value N. Furthermore, in favorable cases, the fraction γ of bg_i scatter can be determined experimentally or is negligible such that finally the fit histograms g_i from MLE depends only on τ, whereas that from LS depends on two parameters τ and N_g.

The convolution in eq 9 is computed numerically between the channels 0 to l using a recursion formula starting at $j = 1$ for the channel $1-k$ according to eq 10.

$$\mathrm{irf}_i \otimes \mathrm{e}^{iT/k\tau} = \sum_{j=1}^{\min(i,l)} \mathrm{irf}_j \mathrm{e}^{-(i-j)T/k\tau} + \sum_{j=i+1}^{k} \mathrm{irf}_j \mathrm{e}^{-(i+k-j)T/k\tau} \tag{10}$$

The second term in eq 10 considers the case of excitation with a high repetition rate of the laser, where the decay time window T is larger than the time between subsequent laser pulses and the signal decay consists of a superposition of decay function with shifted starting times nT.

FLUORESCENCE DECAY ANALYSIS

The instrument response function irf_i (fwhm = 420 ps) was measured with a droplet of a water solution of erythrosine. Since the lifetime of erytrhosine (87 ps) is sizeably shorter than the specified time resolution of the APD detector (>350 ps), this method gives a good representation of the irf. The scatter background bg_i was obtained either by sampling 128 decays of a nondoped polymer film under the same experimental conditions as the sample or by averaging the obtained decays after the bleach of the molecule under study. In both variants, bg_i is normalized to the measurement time of the sample decay to be analyzed. To reduce the number of fit parameters ν for the minimization procedure, the use of the fitting parameter γ for the relative scatter/background contribution is avoided. For all high-level decays, the results with γ fixed to zero were the same as those with floating γ (all obtained values smaller than 2%). However, decays (nine very low level decays, vide infra) obtained with a count rate that is less than 2 times the count rate of the background were corrected by subtraction of the respective bg_i profiles. We verified that the lifetimes obtained by fitting the raw decays using eq 9 with floating γ are the same as those obtained by fitting the background-subtracted decays using eq 9 with $\gamma = 0$. The differences of both lifetimes are statistically distributed with a standard deviation of less than 200 ps. Because of the fact that the ${\chi_r}^2$ and $2I_r^*$ values obtained for these nine very low level decays are statistically not correct, they are not used in the distributions of Figure 4. Finally, since γ was fixed to zero for the analysis of all decays, the constant background values c could directly be obtained by averaging the counts of the first five channels before the rise of the fluorescence decay curve, yielding values in the order of 1−3.

(43) In fact, the use of the scatter parameter γ in the model function g_i of eq 9 would yield $\nu = 2$ for MLE and $\nu = 3$ for LS.

(44) McCullagh, P.; Nelder, J. A. *Generalized Linear Models*; Chapman and Hall: London, 1983.

Chart 1. Spectroscopic Setup Used for the TCSPC Measurements of Single-Molecule Fluorescence Decays Based on a Sample Scanning, Far-Field, Confocal Epifluorescence Microscope

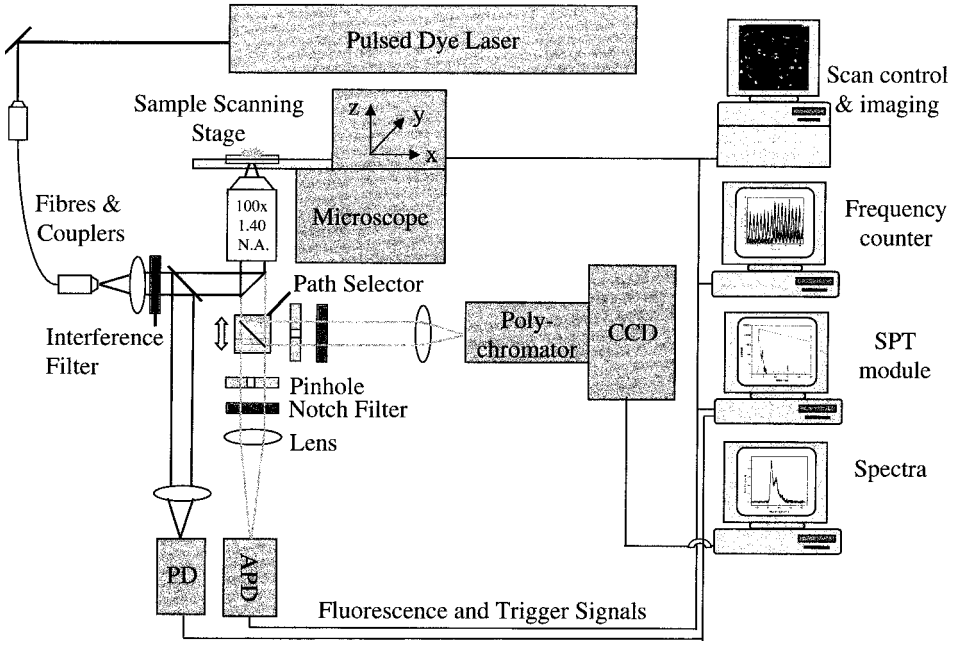

To obtain the fit histogram g_i (eq 9) by the LS fit method, the recorded irf was convoluted with a single exponentially decaying function by fast Fourier transformation and fitted to the experimental decay histogram n_i using the iterative Levenberg−Marquard χ_r^2 minimization routine implemented in the ORIGIN 5.0 PROFESSIONAL (Microcal) program. The MLE fit algorithm is performed using a home-built routine which runs under LABVIEW 5.1 (National Instruments). Here, the convolution in eq 9 is computed numerically using the recursion formula in eq 10 and the minimization is done by a linear parameter screening algorithm.[45] All corresponding LS and MLE fits have been performed with the same noninteger timeshift for the irf, $k = 180$ channels, and a time increment of 0.14 ns/channel, and their quality have been judged by the values of χ_r^2 and $2I_r^*$, respectively, as well as by the residuals and their autocorrelation functions.

EXPERIMENTAL SECTION

The sample preparation of hexaphenylbenzene−perylenemonoimide (for synthesis, see ref 46) imbedded in a poly(vinylbutyral) polymer film of 10−30-nm thickness was done by spin-coating (3500 rpm) 10^{-9} M solutions of the dye in chloroform (Aldrich) mixed with 3 mg/mL poly(vinylbutyral) (Agfa Gevaert). Cover glasses were used as substrates and were cleaned by sonicating in acetone, sodium hydroxide (10%), and MilliQ water, respectively. This procedure yields less than 0.4 molecules/μm^2 in a fluorescence image.

The spectroscopic setup is shown in Chart 1. The output of a pyromethene (Exciton) dye laser pumped by a beam-locked argon ion laser (514 nm) was used as excitation source at a repetition frequency of 4.1 MHz and at a selected wavelength of 543 nm.[47] Using an objective lens (20×, NA 0.4, Newport), the laser light was coupled into a 70-m-long single-mode fiber which after outcoupling with an equivalent lense delivered pulses of less than 20-ps (fwhm) duration and an average power of 5 mW. Passing a beam splitter a part of the light was focused onto a photodiode (Newfocus) to obtain the trigger pulses. A $\lambda/2$ waveplate was used after a linear Glan-Thomson polarizer (Newfocus) to adjust the linear excitation polarization and a $\lambda/4$ waveplate was additionally introduced to obtain the circularly polarized light. The 4 μW of light entered a confocal fluorescence, sample scanning microscope (Nikon, Diaphot 200 microscope in conjunction with a Topometrix scanner) through a dichroic beam splitter (Chroma, 543 nm) and an oil immersion objective lens (100×, NA 1.4) resulting in an excitation power of 600 nW at the sample. The fluorescence is collected with the same lens, passes the beam splitter, a notch filter (Notch Plus 543.5, Kaiser Optics), and a pinhole of 80 μm and is finally detected by a single photon counting Avalanche photodiode (APD; AQ151, Serial 3712, EG&G). To check for impurity fluorescence, a mirror could be slid in to record fluorescence spectra with a cooled (77 K) CCD camera (LN/CCD-512SB, Princeton Instruments). The single photon counting signals of the APD were split: One part was collected in a frequency counter PC card (Keithley, CTM-05/A) to obtain the fluorescence intensity trajectory with a binning time of 10 ms (not shown), and the other was acquired in a time-correlated single photon counting (TCSPC) PC card (SPC 430, Picoquant GmbH) together with the trigger signal to record the fluorescence decays of the single molecule in continuous steps of 10 s.

RESULTS AND DISCUSSION

Typical fluorescence intensity trajectories (time traces) of the hexaphenylbenzene-perylenemonoimide single molecules in poly-

(45) Brand, L.; Eggeling, C.; Zander, C.; Drexhage, K. H.; Seidel, C. A. M. *J. Phys. Chem. A* **1997**, *101*, 4313−4321.

(46) Gensch, T.; Hofkens, J.; Herrmann, A.; Tsuda, K.; Verheijen, W.; Vosch, T.; Christ, T.; Basché, T.; Müllen, K.; DeSchryver, F. C. *Angew. Chem., Int. Ed. Engl.* **1999**, *38*, 3752−3756.

(47) Boens, N. In *Luminescence Techniques in Chemical and Biochemical Analysis*; Baeyens, W. R. G., De Keukeleire, D., Korkidis, K., Eds.; Marcel Dekker: New York, 1991; p 21.

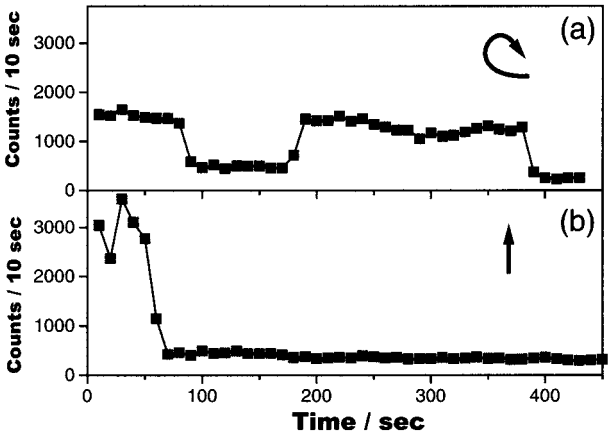

Figure 1. Typical fluorescence intensity trajectories using circularly (a) and linearly (b) polarized 543-nm excitation light.

vinylbutyral polymer films obtained with the TCSPC card are shown in Figure 1 for 543-nm circularly (a) and linearly (b) polarized excitation light. They exhibit the general feature of multiple intensity steps for the circularly polarized excitation, in contrast to a high initial intensity level followed by a comparable fast drop to the background intensity due to photobleaching for the linearly polarized excitation.

The linear polarization of the exciting beam allows a very efficient absorption in the case of parallel orientation of the light and transition dipole moment vector, respectively. Hence, a high number of fluorescence counts can be collected within a short initial time followed by the abrupt photobleaching. On the other hand, excitation by circularly polarized is less efficient and therefore the fluorescence counts are spread over a longer time period. Steps between different fluorescence count levels are likely due to reorientional dynamics either of the fluorescent molecule itself or of the surrounding polymer side chains. Because such processes can alter the fluorescence lifetimes, only the counts of constant fluorescence intensity levels are binned together to obtain the corresponding fluorescence decay curves by adding all its 10-s decays, each of them consisting of $k = 193$ channels in a time window of $T = 27$ ns.

However, decays for analysis were considered only for those levels, that fulfill the two boundary conditions: (1) The total counts N are more than 2500, and (2) the corresponding intensity level of the intensity trace is twice as high as the background level. This filtering should minimize the distortion of the decays by impurity emission and scatter light. By this way, four differently high fluorescence levels have empirically been distinguished (400−1500, 1500−2500, 2500−3500, and 3500−6000 counts/10 s). In the last region of the time trace (after the photobleaching of the molecule), the decay histogram of the background level contains 200−400 counts/10 s decay. This intensity and the decay profile are equal to that of a "dark" blank region due to residual scatter, background fluorescence, and dark noise. Among all decays, nine of the very low levels (400−1500 counts/10 s) obtained with linearly polarized excitation light needed to be corrected by a scatter (bg_i) subtraction, because otherwise the relatively large distortion by scattered laser photons would not have been allowed to fix γ to zero but would yield γ values (eq 9) from 15 to 40% for the raw decays.

As examples, the decays for the initial levels of Figure 1 are plotted in Figure 2 in conjunction with the residual, autocorrelation, and monoexponential fit curves obtained from the LS and the MLE analysis. These decays are representative for an intermediately high (Figure 2a, b), a very low (Figure 2c, d), and a very high (Figure 2e, f) fluorescent level. As expectable for good fits, the residual and autocorrelation functions are randomly distributed around zero with small amplitudes. The monoexponential decay model was sufficient for all decays because the use of a biexponential model resulted in two equal decay times. The fits in Figure 2 also demonstrate that the lifetimes derived from the MLE method are longer than those from the LS method independent of the fluorescence intensity level.

Altogether, 71 decays were analyzed which contain $N = 2500-60\,000$ total counts corresponding to 60−1300 counts in the maximum. To ensure that the analysis of the fluorescence lifetimes is not artificially affected by the number of counts N per decay or the level of counts per 10 s, different plots of the decay analysis parameters versus, for example, level counts, counts of the maximum, or total counts (for the latter, see Figure 3) verify that such a correlation does not exist. It is noteworthy that the results for those nine decays (using linearly polarized laser light) of the very low intensity level (i.e., the level of counts per 10 s close to the minimum limit to be 2 times higher than that of the background level after photobleaching; vide supra) where a scatter correction was applied are equally distributed, confirming that the lifetimes derived by this crucial procedure are reliable, too.

It is important to note, that time-resolved anisotropy measurements showed that within one intensity level of time traces such as in Figure 1 the probe molecules are fixed in the polymer film.[48] Thus, there are no time-dependent contributions due to molecular rotation that distort the fluorescence decay; i.e., the decay is monoexponential irrespective of its orientation and polarization.

The good quality of both monoexponential LS and MLE fitting procedures is demonstrated in Figure 4 by the histograms of χ_r^2 and $2I_r$*. The distributions of both quality parameters are closely distributed around the theoretical expectation value of unity with similar standard deviations.[49] However, the fact that the fit quality parameters of LS are slightly below 1 indicates an improper weighting of the LS method.

Comparing the distributions obtained with linearly and circularly polarized excitation light, respectively, it is obvious that the distributions of the fitting parameters for linearly polarized light are sharper and centered at a slightly lower value indicating somewhat better statistics. This is reasonable, because with linear polarization the fluorescence decay is collected in a shorter macrotime which results, on one hand, in a larger count rate, i.e., a larger signal-to-background ratio preventing a sizable contribution of disturbing fluorescence from the environment or of scatter and, on the other hand, in less fluorescence lifetime broadening induced by environmental fluctuations on a time scale faster than the measurement of a single decay (10 s).

(48) Hofkens, J.; Maus, M.; Gensch, T.; Vosch, T.; Cotlet, M.; Köhn, F.; Herrmann, F.; Müllen, K.; De Schryver, F. C. *J. Am. Chem. Soc.* **2000**, *122*, 9278−9288.

(49) The quality parameters for the nine decays that are treated by the scatter subtraction cannot be used because the noise is no longer Poisson distributed after this procedure.

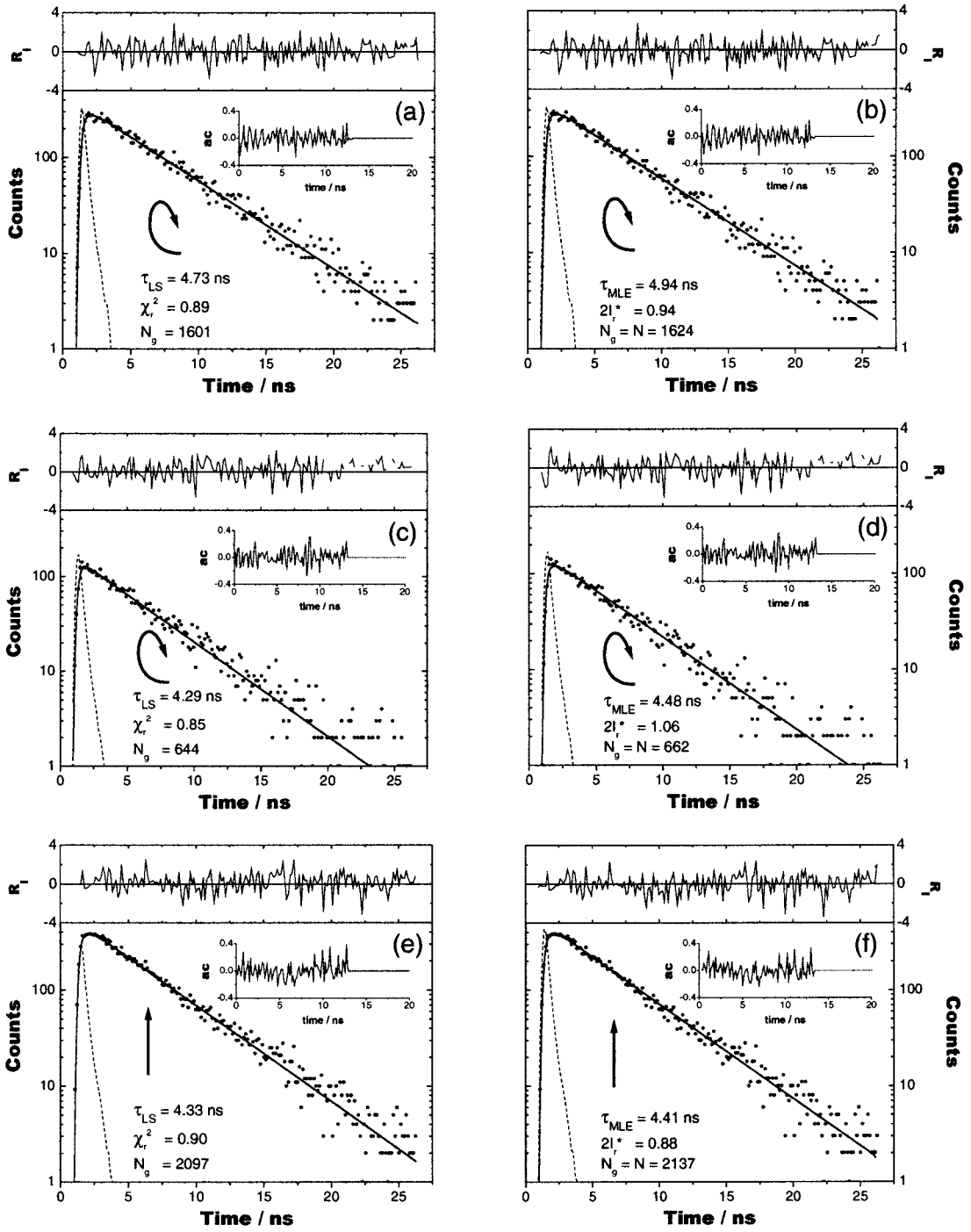

Figure 2. Examples of fluorescence decays corresponding (a−d) to the two initial levels (0−80 and 80−180 s) of the time traces in (1a) and (e, f) corresponding to the initial level (0−60 s) in (1b). The residual, autocorrelation and monoexponential fit curves obtained from the LS and the MLE analysis are also given.

Figure 5 reveals that the obtained mean values and widths of the distributions of the lifetimes are independent of the excitation polarization. This is consistent with excitation and emission of the same first excited singlet state from single hexaphenylbenzene−perylenemonoimide chromophores and confirms that the derived lifetimes are independent of excitation polarization as well as of the collection macrotime. It is interesting to note that the obtained standard deviations σ of the τ distributions of the order of 350 ps are significantly larger than the statistically expected value of the order of 150 ps for a mean $N = 1000$ as derived from eq 11.[15,21] This points directly to the microheterogeneity of the individual dye environments in the investigated sample which can be expected for the inhomogeneous polymer matrix used.

$$\sigma^2 = \frac{\tau^4 k^2}{NT^2}(1 - e^{-T/\tau})\left(\frac{e^{T/k\tau}(1 - e^{-T/\tau})}{(e^{T/k\tau} - 1)^2} - \frac{k^2}{(e^{T/\tau} - 1)}\right)^{-1} \quad (11)$$

Furthermore, the comparison of the mean lifetime obtained by LS with respect to those by MLE indicates lower values for

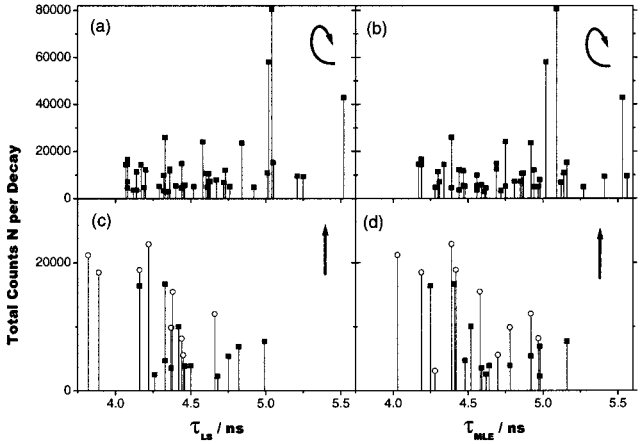

Figure 3. Counts per analyzed decay against the lifetimes derived by the LS and MLE methods for circularly (a, b) and linearly (c, d) polarized excitation light, respectively. Closed squares represent the data from intensity regions without scatter distortion, and the open circles correspond to data that have been corrected for the scatter contribution.

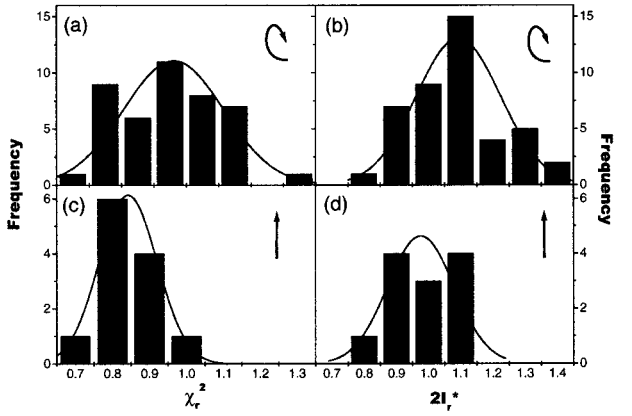

Figure 4. Histograms of χ_r^2 and $2I_r^*$ obtained by the LS and MLE methods for circularly (a, b) and linearly (c, d) polarized excitation light (very low levels in (c) and (d) are excluded). The lines correspond to fitted normal distributions associated with the mean values and standard deviations: (a) 1.01 ± 0.15, (b) 1.09 ± 0.13, (c) 0.84 ± 0.08, and (d) 0.98 ± 0.10.

the LS method. To clarify that such a correlation indeed exists for each analyzed decay, the MLE lifetimes are plotted versus the LS lifetimes in Figure 6.

A straight line can be fitted to these data with a good correlation coefficient of 0.96 and an intercept of 0.21 ns. Consequently, the MLE method estimates the lifetimes 5% larger than the LS method. The reason for this systematic deviation can mainly be traced back to the more appropriate weighting and fitting of the decay channel region with only a small number of counts (tail of the decay) by MLE. This could be proven by fitting the "total decay", being the sum of all circularly and linearly polarized decays, respectively, with the LS and MLE method. Both methods result in the same lifetimes of 4.7 and 4.6 ns for circular and linear polarizations, respectively. Consequently, these lifetime values are in perfect agreement with the mean values of the MLE lifetime distribution for the SM decays in Figure 5, demonstrating the goodness of the MLE fit procedure in the case of a low number of counts.

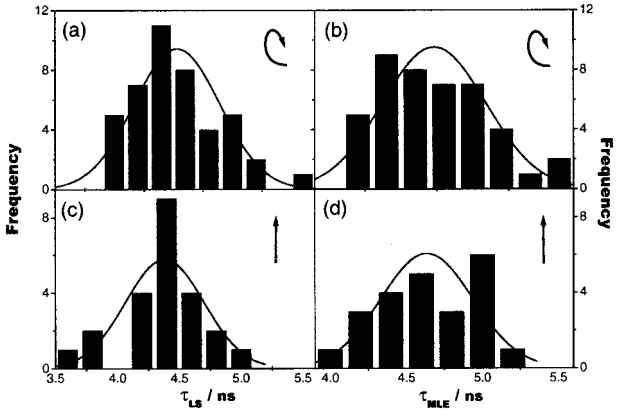

Figure 5. Histograms of the derived lifetimes obtained by the LS and MLE methods for circularly (a, b) and linearly (c, d) polarized excitation light. The lines correspond to fitted Normal distributions associated with the mean values and standard deviations: (a) 4.53 ± 0.36, (b) 4.73 ± 0.36, (c) 4.38 ± 0.32, and (d) 4.63 ± 0.30 ns.

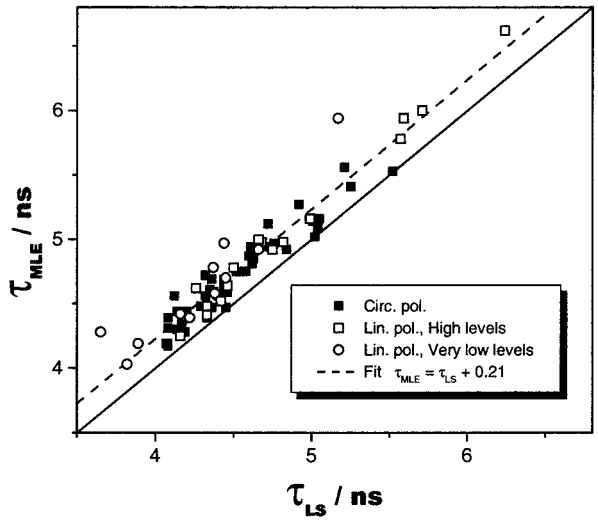

Figure 6. Correlation plot of the lifetimes obtained from the MLE and LS analysis. Open square symbols represent data of highly fluorescent levels and circles of very low levels. Closed square symbols correspond to data with circular excitation polarization, and closed and open circles represent data for linear excitation polarization with and without scatter subtraction, respectively. The full line represents the case of $\tau_{LS} = \tau_{MLE}$, and the dashed line corresponds to the linear fit of all data points with an offset of 210 ps.

To investigate at which number of counts both analysis methods give equivalent results, the ratio of the obtained lifetimes by MLE relative to that of the LS method are plotted in Figure 7a against the number of counts in the respective decays. This kind of scatterplot resembles those plots of fit parameters, such as the anisotropy, versus burst sizes obtained from SM fluorescence bursts.[19,50] With increasing number of counts, hence, increasing information, the uncertainty of the fit parameter, in this case that of the LS lifetime τ_{LS}, decreases. One can see that for a very small number of counts the scatter is rather large, i.e., being between 1.00 and 1.18 for ~2500 counts/decay. With increasing counts, the agreement between the MLE and LS lifetimes becomes better, reaching the plateau of unity at 25 000 counts with a scatter between 1.00 and 1.02.

(50) Taekjip, Ha.; Laurence, T. A.; Chemla, D. S.; Weiss, S. *J. Phys. Chem.* **1999**, *103*, 6839−6850.

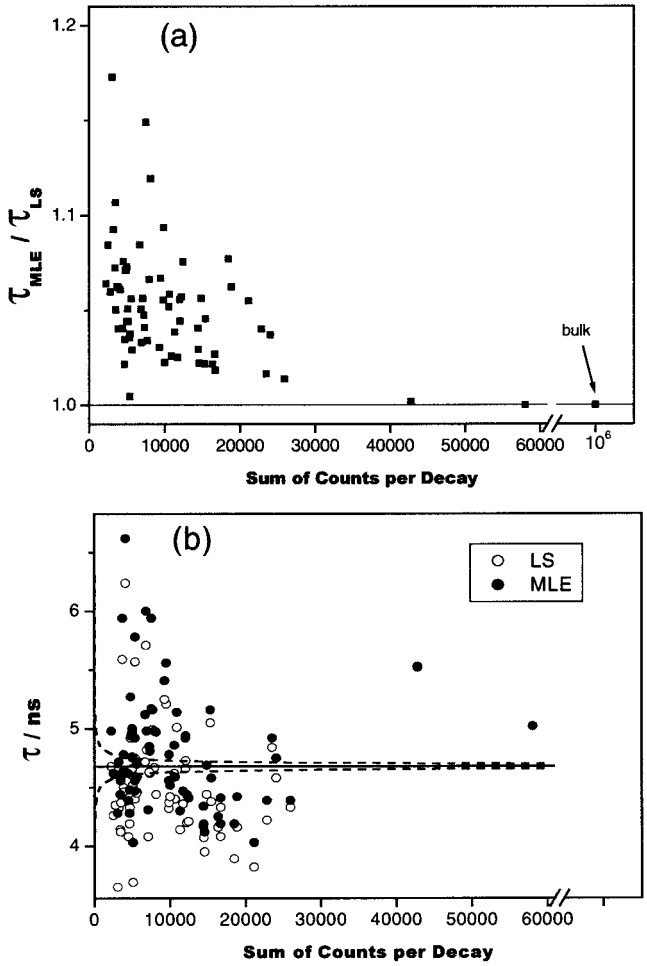

Figure 7. (a) Ratio of analyzed MLE to LS single-molecule lifetime plotted against the sum of counts per analyzed decay. (b) Analyzed MLE (closed circles) and LS (open circles) single-molecule lifetimes plotted against the sum of counts per analyzed decay, respectively. The theoretical standard deviation expected for a single decay time of 4.7 ns as calculated by eq 11 is plotted as a dashed line.

On the other hand, the plot of the analyzed lifetimes versus the number of collected counts in Figure 7b shows a spread for both methods which is clearly larger than expected for only statistical deviations according to eq 11. This spread around the mean value is not a result of the uncertainty of the analysis method, as will be shown below, but reflects the real dependence of the fluorescence lifetime on the inhomogenuous environment. It is known that the decay times of single molecules fixed in 20-nm thin polymer layers[24,28] or adsorbed on a glass surface[51] can deviate strongly from the mean of many molecules. The observed lifetime inhomogenity of the sample on the single-molecule level can be induced by different effects such as different polymer phases, different local polarity and polarizability, different interfaces (polymer−glass, air−polymer) with varying refractive index differences, or different interactions with the dielectric surface dependent on the molecular orientation and distance to the surface. Accordingly, the plot in Figure 7b demonstrates the capability of SM experiments to probe nanosize environments such as interfaces between microsize materials. This is not possible by bulk measurements, because the small contribution of the extreme lifetimes can only be observed by the SM experiments. As a consequence of this lifetime broadening, the

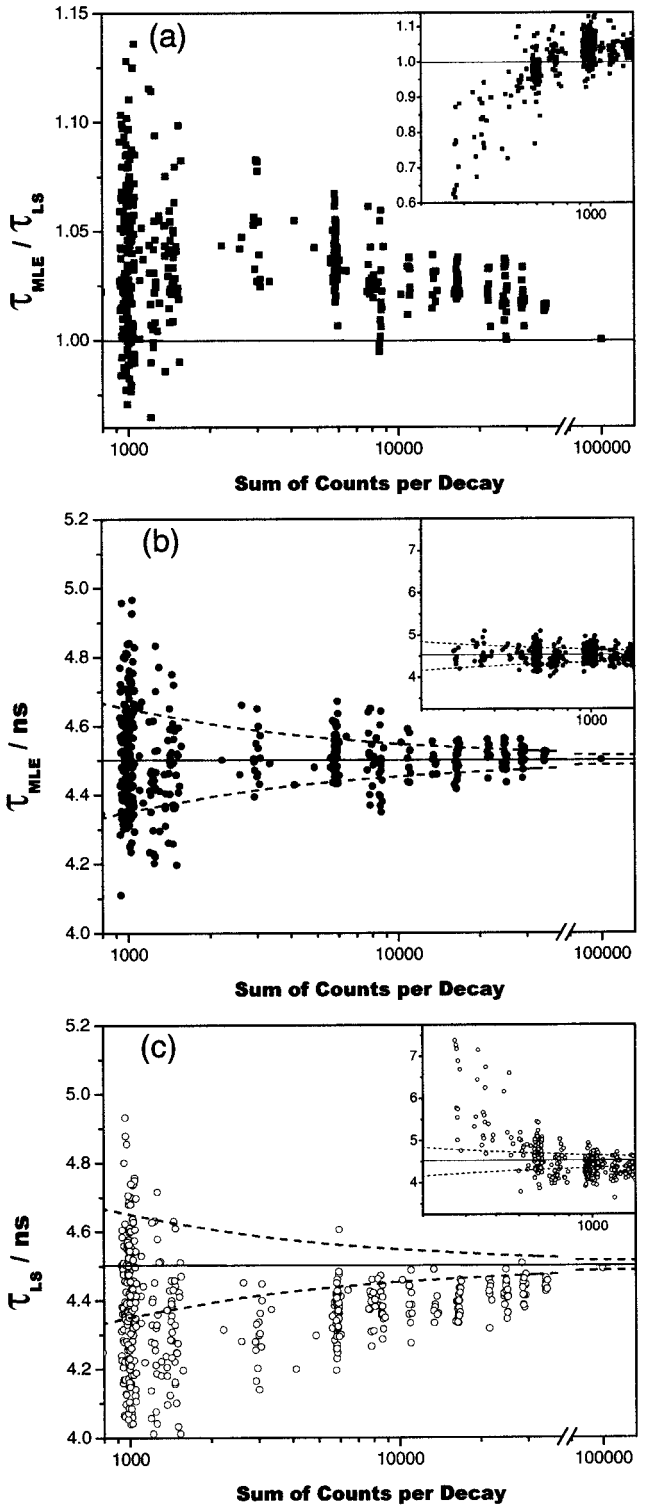

Figure 8. (a) Ratio of analyzed MLE to LS bulk lifetime plotted against the sum of counts per analyzed decay. (b) Analyzed MLE (closed circles) and (c) LS (open circles) bulk lifetimes plotted against the sum of counts per analyzed decay, respectively. The theoretical standard deviation expected for a single decay time of 4.5 ns as calculated by eq 11 is plotted as a dashed line. The insets are zooms of the same plots into the total count regions from 200 to 1500.

(51) Tinnefeld, P.; Buschmann, V.; Herten, D.-P.; Han, K.-T.; Sauer, M. *Single Mol.* **2000**, *1*, 215−223.

lifetimes of single molecules do not necessarily approach the mean lifetime with increasing number of counts.

To avoid this problem of inhomogenuous lifetime broadening and to check not only the statistical difference but also the absolute correctness of the two analysis methods in the absence of the inhomogeneous broadening in case of SM decays, we measured and analyzed ∼600 decays of a 10^{-6} M bulk solution of the fluorophore in ethyl acetate (Figure 8). In this case, the known theoretical lifetime for all the decays is always the same, independent of the measurement time and independent of the number of counts, because the decays are always a result of an ensemble measurement. The number of total counts per decays range mainly from 300 to 40 000 and the fluorescence lifetime determined for 10^9 counts with MLE and LS is in both cases exactly 4.5 ns. The standard deviations for the obtained lifetime distributions for certain number of total counts are in perfect agreement with the theoretically expected values from eq 11, e.g., 150 ps for 1000 counts and 55 ps for 5000 counts. This ensures that the deviations of the analyzed lifetimes from the expected value are purely due to the statistical error of the respective method applied.

In Figure 8a, the ratios of the MLE vs LS analyzed lifetimes are plotted similarly to those in Figure 7a for the SM analyzed lifetime ratios and it can be seen that for the same count region the deviation approaches also to 5% at ∼1000 counts/decay as obtained for the SM analysis. Hence, it is verified that the plot of the analyzed lifetime ratios in Figure 7a only reflects the difference of the two analysis methods. In Figure 8b and c, the homogeneous bulk lifetimes as obtained by MLE and LS analysis, respectively, are also plotted for the same count region. Latter plots visualize directly that LS underestimates the lifetimes for the region between 1000 and 20 000 counts, while that of the MLE gives stable results within the theoretically expected statistical deviation (eq 11) around the correct mean value of 4.5 ns.

In addition, the insets in Figure 8 show the same plots for the region between 300 and 1000 counts/decay, proving that MLE still gives stable results over the whole region while the LS method breaks down as revealed by the large spread and the "inversed behavior" compared to the higher count region; i.e., the LS analyzed lifetimes become larger than the MLE lifetimes with decreasing counts below $N = 1000$.

CONCLUSION

Two TCSPC fluorescence decay analysis procedures based on the weighted least-squares and the maximum likelihood estimation method are elaborated and their results are compared for the mainly investigated count range of $N = 4000-17\,000$ total photons. The key observation of this comparison is that the LS systematically underestimates the fluorescence lifetimes by ∼5%, if only this number of registered events is analyzed, whereas the MLE method gives stable results over the whole intensity range, even at counts N less than 1000, where the LS analysis delivers unreasonable values.

While theoretical studies predict that LS and MLE result in different model parameters at a low number of counts, the present study based on experimental SM decays quantitatively shows that the lifetime results become equivalent at a relatively large number (∼20000) of counts per decay. Since a correlation of decay times (and the ratios of MLE vs LS decay times) with the number of counts per decay, the background or scatter contribution (by checking with and without variable fractions γ of bg_i), the excitation polarization, or the intensity level is not observed, we are confident that the observed deviations between MLE and LS results on SM data are not affected by experimental circumstances. However, this study also directly proves the inhomogenity of the photophysical behavior of single molecules embedded in a thin polymer layer, since the distribution of the derived lifetimes is larger than the statistical standard deviation and the standard deviation for the distribution of the analyzed bulk lifetimes.

The comparison of the distribution of the SM lifetimes with the lifetime of the summed decays as well as the analysis of the bulk decays as a function of the counts renders the MLE method to be the more precise one for a low number of counts (below 20 000). Even though the LS analysis delivers stable decay times as demonstrated by the linear relationship between the LS and MLE lifetimes in Figure 6, for the absolute LS lifetime, the systematic negative mean deviation of 5% in the count range of 4000−17 000 counts N in a decay, which we also found for other single molecule and ensemble fluorescence lifetime studies, should be taken into account. It is therefore recommended to switch from the LS to the MLE method for less than 15 000 total counts/decay. Even if χ_r^2 minimization routines are easily available, it is important for correct decay analysis with low count numbers to apply routines based on $2I_r$*.

The superior performance of MLE over LS in analyzing low signal-to-noise fluorescence decays as found experimentally here is not only important for single-molecule spectroscopy but for all other low signal applications of time-resolved fluorescence spectroscopy. A prominent one is fluorescence lifetime imaging (FLIM), where the analysis is often based on a linear tail calculation or the LS method,[52,53] while MLE fitting has only recently been applied for FLIM, however, considering only the decay tail without deconvolution.[51] As shown here, the use of MLE decreases the amount of detected photons needed for a very precise fluorescence lifetime determination by 2 orders of magnitude. Therefore, the use of MLE offers the possibility to use faster fluorescence scan times, lower excitation energies (less photobleaching and pileup distortion), and lower dye concentrations.

ACKNOWLEDGMENT

M.M. acknowledges the postdoctoral fellowship of the EC through the TMR-SISITOMAS project. J.H. thanks FWO for a postdoctoral fellowship. M.C. is grateful to the KU Leuven for an IDO research fellowship. The additional financial support by the FWO, the EC through the TMR Sisitomas, the SMARTON the VW Stiftung and DWTC (Belgium) through IUAP-IV-11 is gratefully acknowledged.

Received for review July 31, 2000. Accepted January 31, 2001.

AC000877G

(52) Draaijer, A.; Sanders, R.; Gerritsen, H. C. In *Handbook of Biological Microscopy*, 2nd ed.; Pawley, J. B., Ed.; Plenum Press: New York and London, 1995; p 491.

(53) Ghiggino, K. P.; Harris, M. R.; Spizzirri, P. G. *Rev. Sci. Instrum.* **1992**, *63*, 2999−3002.